Mg-doped WO_3 as a novel photocatalyst for visible light-induced water splitting

Dong Won Hwang [a], Jindo Kim [a], Tae Jin Park [b], and Jae Sung Lee [a,*]

[a] Department of Chemical Engineering and School of Environmental Science and Engineering, Pohang University of Science and Technology (POSTECH), San 31 Hyoja-dong, Pohang 790-784, Republic of Korea

[b] Clean Technology Research Center, Korea Institute of Science and Technology, 39-1 Hawolkok-dong, Sungbuk-gu, Seoul 136-791, Republic of Korea

Received 30 October 2001; accepted 23 January 2002

Mg-doped WO_3 with band gap energy of about 2.6 eV is a viable photocatalyst for visible light-induced water splitting in the presence of hole scavengers. The conduction band edge position of p-type Mg-doped WO_3 was −2.7 V *versus* SCE at pH 12. By doping Mg on WO_3, the conduction and valence band positions were shifted by 2.25 V negatively, leading to a conduction band edge position which was negative enough for H^+ ions to be reduced thermodynamically, with little change in band gap energy. The negative shift in band position might be ascribed to lowering of the effective electron affinity of WO_3 by doping Mg with a very low electron affinity.

KEY WORDS: Mg-doped WO_3; photocatalyst; visible light; water splitting; band position shift.

1. Introduction

Production of hydrogen from decomposition of water using solar energy has been considered an ultimate technology to solve both energy and environmental problems resulting from current use of fossil fuels. An efficient photocatalyst is needed for the technology to work. Although there has been remarkable progress in the last decades for photocatalysts working under ultra-violet light [1–4], this progress has rarely been extended to visible light. The first requirement for visible light-induced photocatalyst is the proper band gap energy. However, only a few materials of photocatalytic activity satisfy this condition, such as CdS, WO_3 and Fe_2O_3. Although CdS is a good candidate for photocatalytic water reduction, it has a fatal photocorrosion problem in that CdS itself is oxidized by the photogenerated hole. Kudo and Sezikawa have reported some CdS-based photocatalysts modified by Cu-ZnS or Ni-ZnS [5,6], over which H_2 was produced from H_2O in the presence of sacrificial agents such as Na_2S and methanol. Although WO_3 and Fe_2O_3 have proper band gaps for visible light absorption, these materials could not be used in photocatalytic water reduction due to the improper conduction band edge position relative to the reduction potential of water [7]. There were few reports on non-sulfide-type photocatalysts that produce hydrogen from water under visible light. In search of an oxide photocatalyst working under visible light, we discovered that modification of WO_3 by doping with MgO gave interesting photocatalytic properties. In this paper, we report Mg-doped WO_3 as a novel non-sulfide, visible light-induced photocatalyst, over which H_2 evolves photocatalytically in the presence of a sacrificial agent.

2. Experimental

Mg-doped WO_3 was prepared by an impregnation method: WO_3 (Aldrich 99.99%) was added to an aqueous solution containing a required amount (5–20 wt% of powder) of $Mg(NO_3)\cdot 6H_2O$ (Aldrich) and then water was evaporated in a rotary evaporator. Mg-doped WO_3 was calcined at 773 K in air for 3 h, ground in a mortar, pelletized and then sintered in a platinum crucible at a temperature between 1173 K and 1523 K for 17 h. The Pt deposition on Mg-doped WO_3 was performed by photoplatinization; 0.05 g of H_2PtCl_6 was introduced into the reaction system (EtOH 50 ml + distilled water 300 ml) containing 1 g of catalyst, and then 2 h of UV irradiation through a Pyrex filter was conducted. Photocatalytic reaction was carried out at room temperature in a closed gas circulation system using a high-pressure Hg lamp (Ace Glass Inc., 450 W) placed in an inner irradiation-type Pyrex reaction cell [1,2]. Ultra-violet light (<400 nm) was removed with a solution filter (1 M $NaNO_2$). The catalyst (0.2 g) was suspended in distilled water (350 ml) by magnetic stirring. The rates of H_2 evolution were determined from analysis of the gas phase by gas chromatography (TCD, molecular sieve 5 Å column and Ar carrier).

The crystal structure of the sintered powder was determined by X-ray diffraction (XRD, Mac Science Co., M18XHF) and the band gap energy was measured by

* To whom correspondence should be addressed.
E-mail: jlee@postech.ac.kr

1011-372X/02/0500-0053/0

UV–vis diffuse reflectance spectroscopy (Shimadzu, UV 525). Photoelectrochemical experiments were conducted on an electrochemical cell filled with a NaOH solution, where a Pt counter electrode, a saturated calomel reference electrode (SCE), and a working electrode were immersed. A tungsten halogen lamp provided illumination of the sample through a quartz window, and a band pass filter (<400 nm) removed the UV irradiation.

3. Results and discussion

Bulk structures of synthesized compounds were analyzed by XRD and compared with reference samples of WO_3, MgO and $MgWO_4$ in figure 1. A new phase was observed for 10 wt% Mg-doped WO_3 (B) which was neither WO_3 (A) nor MgO (E). This new phase began to appear by sintering at around 1223 K with a few impurity phases which disappeared when sintered at 1523 K for 17 h. Most peaks of 10 wt% Mg-doped WO_3 overlapped with those of $MgWO_4$ (C) and WO_3, and therefore the structure of 10 wt% Mg/WO_3 appeared to be composed of a mixture of $MgWO_4$ and WO_3. 20 wt% doping of Mg on WO_3 (D) gave an XRD pattern almost identical to that of $MgWO_4$ with some MgO impurity. Figure 2 shows the diffuse reflectance spectra (DRS) of Mg-doped WO_3 and some reference compounds. The color of WO_3 was lime-green, which changed to light pink after doping 10 wt% Mg followed by sintering at 1523 K for 17 h, and then changed to white after 20 wt% doping Mg. The band gap energy (E_g) of Mg-doped WO_3 was estimated to be around 2.6 eV from the absorption edge of around 480 nm, which was nearly identical to that of WO_3. However, the amount of light absorption of 10 wt% Mg-doped WO_3 was only half as large as that of WO_3. On the other hand, $MgWO_4$ (Aldrich) with a spinel structure,

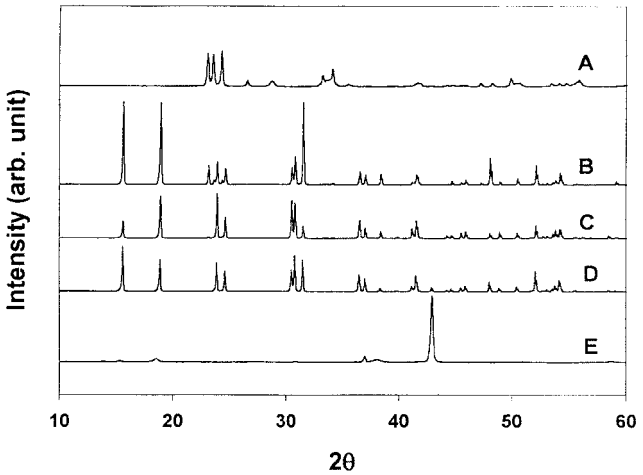

Figure 1. XRD patterns of various oxides. (A) WO_3, (B) Mg(10 wt%)/WO_3, (C) $MgWO_4$, (D) Mg(20 wt%)/WO_3, (E) MgO.

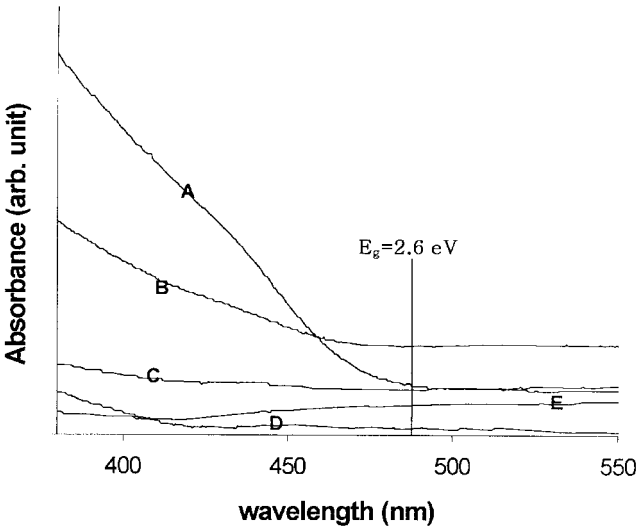

Figure 2. UV-DRS patterns of various oxides. (A) WO_3, (B) Mg(10 wt%)/WO_3, (C) $MgWO_4$, (D) Mg(20 wt%)/WO_3, (E) MgO.

MgO (Aldrich) and 20 wt% of Mg-doped WO_3 did not show any visible light absorption above 400 nm. From this result of UV–vis absorption, 10 wt% Mg-doped WO_3 seems to have a mixed character of $MgWO_4$ and WO_3, which is in agreement with XRD results. Thus, 10 wt% Mg-doped WO_3 could be the best candidate for visible light-induced photocatalyst in water splitting.

Figure 3 shows the amount of H_2 evolution with reaction time over 5 wt% Mg-doped WO_3 in the presence of EDTA as a hole scavenger and NaOH under visible light irradiation ($\lambda > 400$ nm). The solution pH containing 1 g, 2.7×10^{-3} mol of EDTA was about 6 and it became about 12 upon addition of 1 g, 0.025 mol of NaOH. Before photocatalytic reaction, the blank test was performed. No H_2 was produced without catalyst, or without additive (EDTA and NaOH), or without

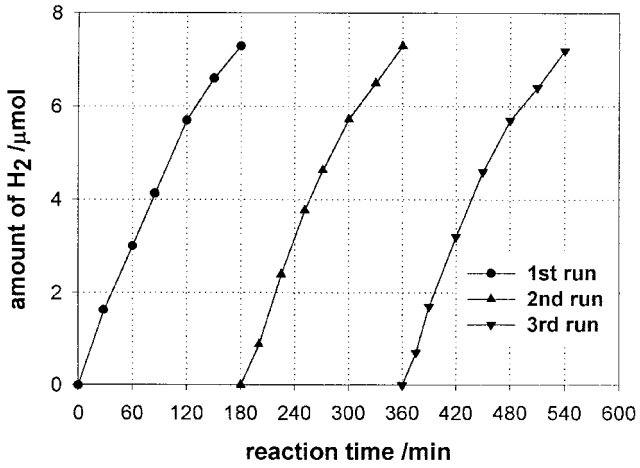

Figure 3. A typical time course of H_2 evolution over Mg(5 wt%)/WO_3 under visible light irradiation ($\lambda > 400$ nm). Reaction conditions: catalyst 0.2 g; distilled water 350 ml; NaOH 1 g; EDTA 1 g; light source: UV irradiation ($\lambda < 400$ nm) of 450 W high-pressure Hg lamp was cut off by 1 M $NaNO_2$.

irradiation. H_2 evolved steadily as light irradiation started and H_2 evolution stopped when light irradiation stopped. The rate of H_2 evolution was slightly decreased with the reaction time. However, the initial activity of 3 μmol/h was recovered after refreshing the reaction system with air as shown in figure 3. The amount of O_2 decreased with reaction time, which might result from further oxidation of the initially oxidized EDTA by photogenerated hole. However, the amount of O_2 in the reaction system did not affect the H_2 evolution rate since the same rate of H_2 evolution was obtained when the reaction system was purged by Ar gas.

Since two electrons are needed to produce a molecule of H_2 from water, the turnover number of hydrogen production with respect to the amount of Mg doped reached 3 at the reaction time of 200 h if all Mg atoms have participated in the water splitting. This confirms that H_2 evolution over Mg-doped WO_3 occurs photocatalytically.

To test the effect of NaOH and hole scavenger, the EDTA was replaced by Na_2S, another widely used hole scavenger. When Na_2S was used as a hole scavenger, the evolution of H_2 occurred even without NaOH. The reactant solution pH containing the same amount (2.7×10^{-3} mol) of Na_2S was also about 12 since Na_2S produced the same amount of NaOH by reaction (1), and further addition of NaOH did not affect the catalytic activity.

$$2Na_2S + O_2 + H_2O \rightarrow Na_2S_2O_3 + 2NaOH. \quad (1)$$

The rate of H_2 evolution was steady and the same as the rate observed when EDTA was used as a hole scavenger together with NaOH. When Pt metal, known to provide electron transfer sites in many photocatalytic reactions, was loaded on 10 wt% Mg-doped WO_3, there was little positive effect on the activity of Mg-doped WO_3.

Table 1 shows the rate of H_2 evolution of various photocatalysts when EDTA was used as a hole scavenger. The H_2 evolution rate of 3 μmol/h did not vary significantly with Mg doping concentration in the range of 5–10%. Outside this level, however, Mg-doped WO_3 had little photocatalytic activity. For comparison with Mg-doped WO_3, the photocatalytic water-splitting reaction over bare WO_3 was also performed. WO_3 did not show any activity of water splitting but itself was decomposed in this highly basic reaction condition. 20 wt% Mg-doped WO_3 showed similar activity to that of $MgWO_4$, which is in agreement with the result by X-ray diffraction shown in figure 1. From the viewpoint of UV–vis DRS in figure 2, 20 wt% Mg-doped WO_3 and $MgWO_4$ should not show any activity since they did not absorb the visible light ($\lambda > 400$ nm). Therefore, a little activity for these catalysts might result from the leakage of UV irradiation ($\lambda < 400$ nm) when 1 M $NaNO_2$ was used as a solution filter for cutting off UV irradiation.

Table 1
Photocatalytic activity of various photocatalysts

Photocatalyst [a]	H_2 evolution rate [b] (μmol h^{-1})
WO_3	0
$Mg(5)/WO_3$	3.0
$Mg(10)/WO_3$	3.0
$Mg(20)/WO_3$	0.2
$MgWO_4$	0.2

[a] The loading (wt%) of Mg is indicated in parentheses.
[b] Reaction condition: catalyst 0.2 g; distilled water 350 ml; NaOH 1 g; EDTA 1 g.

As already mentioned in a previous report [7], WO_3 itself does not produce H_2 from H_2O photocatalytically due to the improper conduction band edge position relative to the reduction potential of H_2O. That is, its conduction band edge is more positive than the reduction potential of H_2O (H_2/H^+). However, the thermodynamic requirement of H_2 evolution from photocatalytic water splitting is to have the conduction band edge of the photocatalyst positioned more negatively than the reduction potential of H^+. We measured the conduction band edge position of Mg-doped WO_3 photoelectrochemically. In heavily-doped semiconductor, the Fermi level (E_F) could be assumed to be the conduction band edge for n-type and valence band edge for p-type. The Fermi level was estimated from the flat-band potential of each semiconductor, which was assumed to be the photocurrent onset potential in the electrolyte of NaOH, since photocurrent is generated only when applied potential (E_{app}) exceeds the flat-band potential (E_{fb}) for an n-type semiconductor ($E_{app} > E_{fb}$), and vice versa for a p-type semiconductor ($E_{app} < E_{fb}$). Figure 4 shows photoresponse of WO_3 (A) and 10 wt% Mg-doped WO_3 (B) at pH 12. WO_3 shows a typical photoresponse (anodic photocurrent) of an n-type semiconductor, while Mg-doped WO_3 shows that of a p-type (cathodic photocurrent). The value of the flat-band potential (photocurrent onset potential, E_{on}) for n-type WO_3 from the photoresponse in figure 4(A) was -0.45 V *versus* SCE, which is in a good agreement with the earlier work (CB level of 0.2 V *versus* SCE at pH 1) [7]. Therefore, H_2O could not be reduced photocatalytically over WO_3, since the reduction potential of H_2O is -0.88 V *versus* SCE at pH 12. The conduction band edge of p-type Mg-doped WO_3 was estimated from the photocurrent onset potential of -0.1 V *versus* SCE at pH 12 in figure 4(B), which corresponded to the valence band edge. With the band gap energy of 2.6 eV, the obtained value of the conduction band edge position was -2.7 V *versus* SCE at pH 12, now a negative enough potential to reduce H^+ to H_2. The change in band position from WO_3 to Mg-doped WO_3 is schematically shown in figure 5. Comparing the conduction band edge of WO_3 and Mg-doped WO_3, the negative shift of 2.25 V was caused by doping Mg on WO_3. However, for the simultaneous evolution of H_2 and O_2, the valence band edge position of 10 wt% Mg-doped WO_3

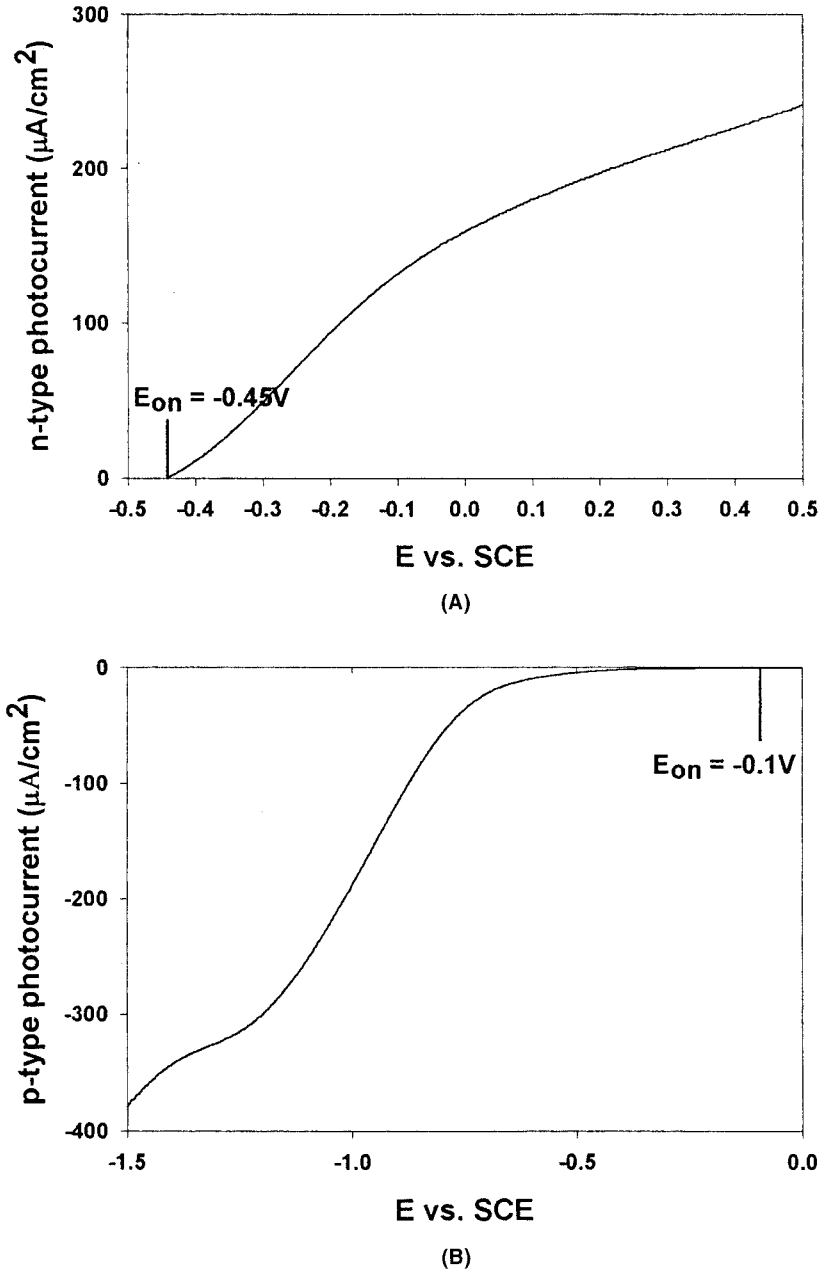

Figure 4. Photocurrent density as a function of applied potential in 0.07 N NaOH (pH 12). (A) WO_3, (B) 10 wt% Mg-doped WO_3. Light source: tungsten halogen lamp ($\lambda > 400$ nm).

should be shifted positively by at least 0.45 V, since H_2O could not be oxidized into O_2 due to its more negative valence band edge position (−0.1 V *versus* SCE) than the oxidation potential of water (+0.35 V *versus* SCE).

In general, the valence band of the transition metal oxide semiconductor is formed by the p orbital of the oxygen anion and the conduction band is formed by the d and/or s orbital of the transition metal cation in the oxide. The conduction band edge of an oxide semiconductor could be mainly determined by the electronegativity (electron affinity) of the element constituting the oxide [8]. Thus, the oxide semiconductor containing an alkaline or alkaline-earth metal with a low electronegativity has a higher band position than the oxide semiconductor without such a dopant because the bandgap of the oxide is determined mainly by the transition metal cation [9]. The bandgap of WO_3 and Mg-doped WO_3 was nearly identical, as shown in UV-DRS patterns in figure 2. The electron affinity (EA) of Mg and that of W is 0 and 78.6 kJ mol^{-1}, respectively [10]. As a result, the conduction band edge position of WO_3 shifted to a more negative level than the reduction potential of H_2O by doping the alkaline-earth metal (Mg) on the transition metal (W). This argument is also reinforced by the similar result of Turner *et al.* [11] that the negative shift (200 mV cathodic shift) of the

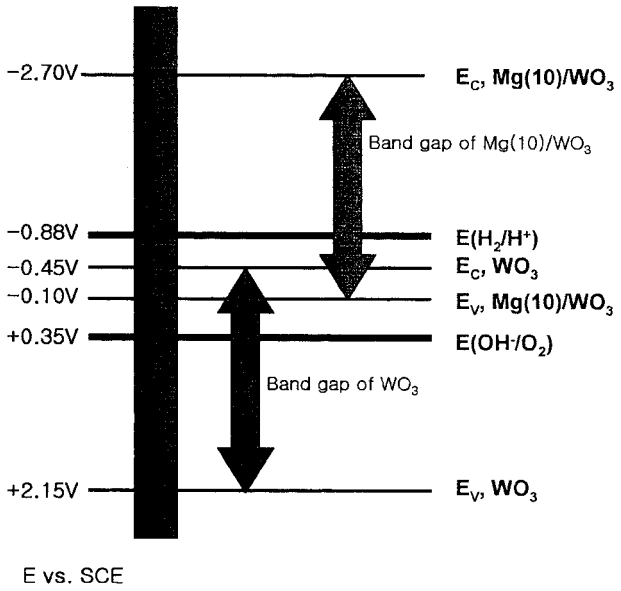

Figure 5. A schematic diagram of conduction and valence band edge positions for p-type Mg(10 wt%)/WO_3 and n-type WO_3.

conduction and valence band edges relative to undoped n-type Fe_2O_3 occurred when Mg was doped on Fe_2O_3. The reason for only a small negative shift of band position might be ascribed to a high electron affinity of Fe (15.7 kJ mol^{-1}) relative to W.

4. Conclusions

Mg-doped WO_3 with a band gap energy of about 2.6 eV showed photocatalytic activity in the water splitting reaction under visible light irradiation ($\lambda > 400$ nm). However, pure WO_3 did not show the photocatalytic activity in strong basic condition due to the improper conduction band edge position. H_2 evolved (3.0 μmol g h^{-1}) continuously by doping Mg (5–10 wt%) on WO_3, although the amount of visible light absorption was diminished. The conduction band edge position of n-type WO_3 was −0.45 V *versus* SCE at pH 12 and that of Mg-doped WO_3 was −2.7 V *versus* SCE. Therefore, by doping Mg on WO_3 the conduction band edge position was shifted by 2.25 V negatively, leading to a conduction band edge position which was negative enough for H^+ ion to be reduced thermodynamically, with little change in band gap energy. The negative shift of conduction band resulted in the steady photocatalytic H_2 evolution.

Acknowledgments

This work was supported by grant 1999-1-307-007-3 from the Basic Research Program of the Korea Science and Engineering Foundation and Brain Korea 21 program.

References

[1] H.G. Kim, D.W. Hwang, J. Kim, Y.G. Kim and J.S. Lee, Chem. Commun. (1999) 1077.
[2] D.W. Hwang, H.G. Kim, J. Kim, K.Y. Cha, Y.G. Kim and J.S. Lee, J. Catal. 193 (2000) 40.
[3] S. Ikeda, M. Hara, J.N. Kondo, K. Domen, H. Takahashi, T. Okubo, and M. Kakihana, J. Mater. Res. 13 (1998) 852.
[4] Y. Inoue, Y. Asai, and K. Sato, J. Chem. Soc., Faraday Trans. 90 (1994) 797.
[5] A. Kudo and M. Sekizawa, Catal. Lett. 58 (1999) 241.
[6] A. Kudo and M. Sekizawa, Chem. Commun. 15 (2000) 1371.
[7] M. Schiavello and A. Sclafani, in: *Photocatalysis; Fundamentals and Applications*, eds. N. Serpone and E. Pelizzetti (Wiley Interscience, New York, 1989) p. 432.
[8] M.A. Butler and D.S. Ginley, J. Electrochem. Soc. 125 (1978) 228.
[9] Y. Matsumoto, J. Sol. State Chem. 126 (1996) 227.
[10] J.E. Huheey, E.A. Keiter, and R.L. Keiter in: *Inorganic Chemistry: Principles of Structure and Reactivity*, 4th edition (HarperCollins, New York, 1993).
[11] J.E. Turner, M. Hendewerk, J. Parmeter, D. Neiman and G.A. Somorjai, J. Electrochem. Soc. 131 (1984) 177.